THE JOURNAL OF PHYSICAL CHEMISTRY Letters

Letter

Cite This: J. Phys. Chem. Lett. 2019, 10, 2143−2150

pubs.acs.org/JPCL

Preferential Binding of π-Ligand Porphyrin Targeting 5′-5′ Stacking Interface of Human Telomeric RNA G-Quadruplex Dimer

Qige Qi,[†,§] Chunfan Yang,[*,‡] Ye Xia,[‡] Shaoshi Guo,[‡] Di Song,[*,†] and Hongmei Su[*,‡]

[†]Beijing National Laboratory for Molecular Science, Institute of Chemistry, Chinese Academy of Science, Beijing 100190, China

[‡]College of Chemistry, Beijing Normal University, Beijing 100875, China

[§]University of Chinese Academy of Science, Beijing 100049, China

Supporting Information

ABSTRACT: Human telomeric RNA (TERRA) containing thousands of G-rich repeats has the propensity to form parallel-stranded G-quadruplexes. The emerging crucial roles of TERRA G-quadruplexes in RNA biology fuel increasing attention for studying anticancer ligand binding with such structures, which, however, remains scarce. Here we utilized multiple steady-state and time-resolved spectroscopy analyses in conjunction with NMR methods and investigated thoroughly the binding behavior of TMPyP4 to a TERRA G-quadruplex dimer formed by the 10-nucleotide sequence r(GGGUUAGGGU). It is clearly identified that TMPyP4 intercalates into the 5′-5′ stacking interface of two G-quadruplex blocks with a binding stoichiometry of 1:1 and binding constant of 1.92×10^6 M^{-1}. This is consistent with the unique TERRA structural features of the enlarged π−π stacking plane of the A·(G·G·G·G)·A hexad at 5′-ends of each G-quadruplex block. The preferential binding of π-ligand porphyrin to the 5′-5′ stacking interface of the native TERRA G-quadruplex dimer is first ascertained by the combination of dynamics and structural characterization.

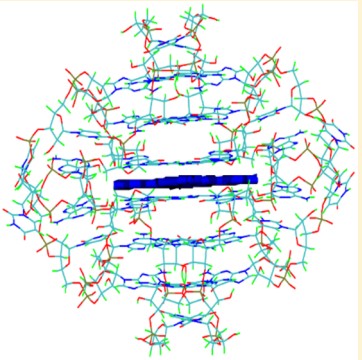

Telomeres are the ends of eukaryotic chromosomes, which fulfill essential functions for chromosome stability. With thousands of 5′-TTAGGG-3′ repeats in its sequence, the human telomere is guanine-rich and can adopt noncanonical four-stranded secondary structures called guanine (G)-quadruplexes, by stacking of planar G-tetrads comprising four guanines via Hoogsteen hydrogen bonds.[1] G-quadruplex motifs are prevalent in genomes. The DNA G-quadruplexes have been proposed to regulate biological functions of telomeres, thereby becoming potential anticancer targets and facilitating development of anticancer agents through synthesis and design of ligands that can stabilize G-quadruplexes.[2]

Over the past few years, accumulating evidence has emerged showing also the inevitable existence of RNA G-quadruplexes in vivo, which are regulators of key cellular functions.[3−5] Telomeric DNA can be transcribed into noncoding RNA termed TERRA (telomeric repeat-containing RNA) that contains thousands of G-rich repeats of 5′-UUAGGG-3′. Studies of NMR spectra, circular dichroism (CD) spectra, and X-ray crystallography[6,7] have shown that these TERRA strands are also able to form stable G-quadruplex structures in the presence of sodium or potassium ions (Na^+ and K^+).[8−10] Many proteins important for telomere maintenance bind to TERRA via the G-quadruplexes. TERRA G-quadruplex mediates functions of regulation and protection of chromosome ends, and, in turn, affects the biological processes of cancer and aging.[11−13] RNA G-quadruplexes are important for telomere biology and can be alternative therapeutic targets for cancer therapy.[14,15] Owing to the biological significance and potential applications in anticancer drug design, studies of ligand binding and ligand design targeting TERRA G-quadruplexes are attracting increasing attention.[10,16,17]

Interactions between G-quadruplexes and ligands are highly associated with structures of G-quadruplexes.[18−22] Structural analysis showed that topologies of TERRA G-quadruplexes are different from corresponding DNA G-quadruplexes, although their sequences differ only in uracil (U) or thymine (T) bases. G-rich DNA sequences can form polymorphic structures depending on the sequences and surrounding factors.[23] For example, the 22-nucleotide (22-nt) four-repeat human telomeric DNA sequence d[AGGG(TTAGGG)$_3$] folds into an antiparallel-stranded G-quadruplex in Na^+ solution and a hybrid (antiparallel/parallel-stranded) G-quadruplex in K^+ solution,[1] while the identical RNA sequence r[AGGG-(UUAGGG)$_3$] folds into only a parallel-stranded G-quadruplex in both Na^+ and K^+ solutions.[9,24,25] Because parallel-stranded G-quadruplexes have a strong propensity for stacking, TERRA G-quadruplexes generally exist in the form of dimers or other higher-order structures.[11,26] However, to date, in contrast to the situation for DNA G-quadruplexes, very few studies on ligand binding with RNA G-quadruplexes have been performed, and even less is known about the ligand binding with TERRA G-quadruplexes.

Received: March 5, 2019
Accepted: April 15, 2019
Published: April 15, 2019

DOI: 10.1021/acs.jpclett.9b00637
J. Phys. Chem. Lett. 2019, 10, 2143−2150

Interestingly, the crystal structure of a TERRA quadruplex–acridine complex was reported, indicating the insertion and stacking of two acridine molecules between two G-quadruplex blocks of TERRA G-quadruplex dimer adopted by the 12-nt r(UAGGGUUAGGGU) sequence.[27] The bimolecular RNA complex has a parallel-stranded topology with propeller-like UUA loops. Upon binding with acridine, there were significant loop conformational changes in the RNA G-quadruplex and the UA at its 5′-ends rearranged greatly compared to the native TERRA G-quadruplex. For this X-ray crystal structure of acridine/quadruplex dimer complex, however, questions were raised by later studies[28] whether this G-quadruplex dimer existed before being crystallized or if the conformation was just induced by acridine ligands. Additionally, an NMR-based solution structure from Phan and Martadinata has established that[9] this 12-nt human telomeric RNA sequence can only fold into G-quadruplex monomer rather than further stacking of two such G-quadruplex blocks into a dimer because the hindrance of the overhang of UA at its 5′-ends prevents stacking. Thus, it will be of great interest to evaluate the binding behavior of ligands targeted to a natively existent TERRA G-quadruplex dimer.

In this Letter, we choose the 10-nt r(GGGUUAGGGU) sequence that can form native TERRA G-quadruplex dimer[28] and is the structural building block of human telomeric RNA ranging from 100 to 9000-nt repeats r(UUAGGG) and study its binding interaction with the cationic 5, 10, 15, 20-tetra (*N*-methyl-4-pyridyl) porphyrin (TMPyP4, see Scheme 1c). TMPyP4 is a prototypical ligand which can strongly bind with DNA G-quadruplexes and act as anticancer agents.[29−32] Its binding interaction with RNA G-quadruplexes, however, is unknown. TERRA G-quadruplex dimer has a well-characterized structure,[28] in which two strands of the 10-nt r(GGGUUAGGGU) form an intermolecular parallel-stranded TERRA G-quadruplex block which then stacks with other blocks at their 5′-ends to form a dimer structure (shown in Scheme 1a). Noticeably, the resulting 5′-5′ stacking interface is composed of two A·(G·G·G·G)·A hexads (see Scheme 1b), where the adenine (A) of UUA linkers is positioned nearly coplanar to the G-tetrad core and its nitrogen atom (N1) is bound to 2′-OH group of the adjacent G1 at the 5′-end. Interestingly, by a thorough study of time-resolved UV−vis absorption spectroscopy in conjunction with NMR, fluorescence, and induced circular dichroism (ICD) spectroscopy, we find that TMPyP4 intercalates into the 5′-5′ stacking interface between two G-quadruplex blocks as the preferential binding site (see Scheme 2), with a strong binding affinity (1.92×10^6 M^{-1}) and 1:1 binding stoichiometry. These results suggest that the enhanced $\pi-\pi$ stacking due to A·(G·G·G·G)·A hexads can enable the 5′-5′ stacking interface to be a favorable site for ligand binding, thus providing mechanistic insights for rational design of drugs targeting higher-order arrangements of G-quadruplexes in long TERRA sequences. We note that the combination of dynamics and structural characterization by time-resolved UV−vis absorption spectroscopy and NMR reveals a clear picture of binding interactions for the first time for the π-ligand porphyrin with the native TERRA G-quadruplex dimer.

Scheme 1. Structures for (a) Side View of the TERRA G-Quadruplex Dimer Formed by the 10-nt TERRA r(GGGUUAGGGU) Sequence, (b) Top View of the A·(G·G·G·G)·A Hexad, and (c) TMPyP4

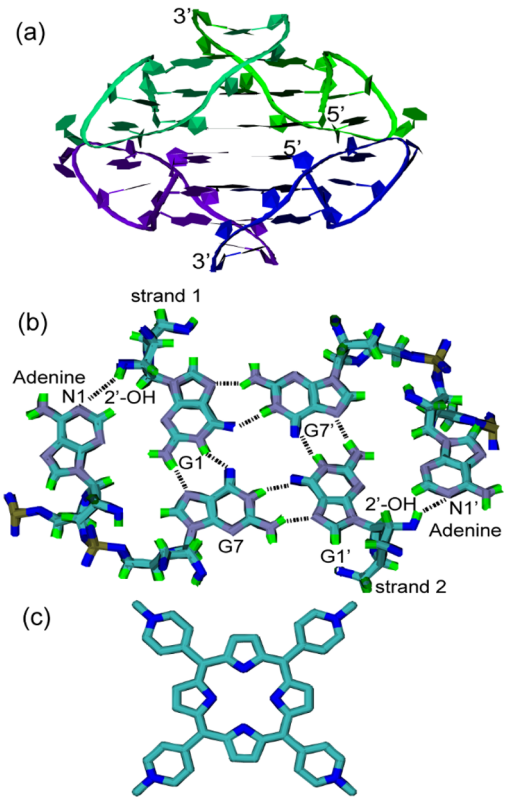

Scheme 2. Depiction of the Intercalation Binding of TMPyP4 at the 5′-5′ Stacking Interface of the TERRA G-Quadruplex Dimer

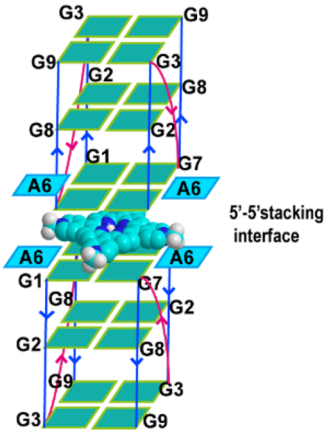

Formation of TERRA G-Quadruplex Structure. According to previous data, the 10-nt TERRA r(GGGUUAGGGU) sequence in K^+ buffer solution can form a parallel-stranded G-quadruplex dimer (Scheme 1a).[28] To confirm the formation of the dimeric G-quadruplex, both CD spectroscopy and gel electrophoresis experiments were carried out. The CD spectrum (Figure 1a) shows a positive peak at 260 nm and a negative peak at 240 nm, which indicates the formation of the RNA G-quadruplex with a parallel-stranded conformation.[9] The molecular size of the G-quadruplex is visualized by nondenaturing polyacrylamide gel electrophoresis. As shown in Figure 1b, the first lane in the gel electrophoresis photograph corresponds to DNA oligonucleotides marker, and the second

DOI: 10.1021/acs.jpclett.9b00637
J. Phys. Chem. Lett. 2019, 10, 2143−2150

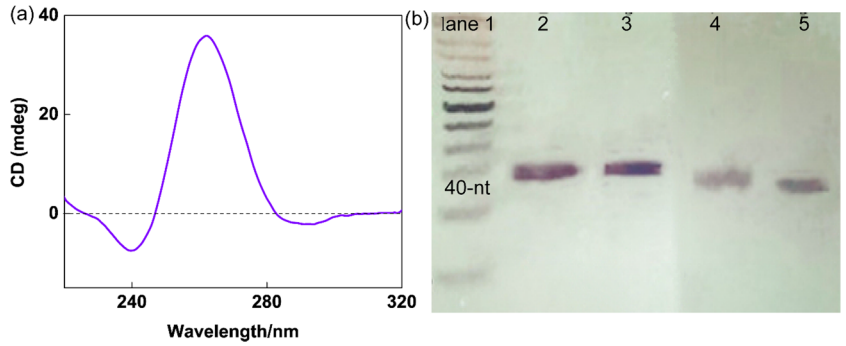

Figure 1. (a) CD spectrum of the 10-nt r(GGGUUAGGGU) sequence (32 μM) forming parallel-stranded G-quadruplex with the TERRA G-quadruplex dimer (8 μM). (b) Polyacrylamide gel analysis of 10-nt TERRA G-quadruplex dimer. Lane 1: DNA marker ladder. Lanes 2 and 3: TERRA G-quadruplex dimer concentration of 10 μM without and with 2 μM TMPyP4, respectively. Lanes 4 and 5: TERRA G-quadruplex dimer of 8 μM without and with 2 μM TMPyP4, respectively.

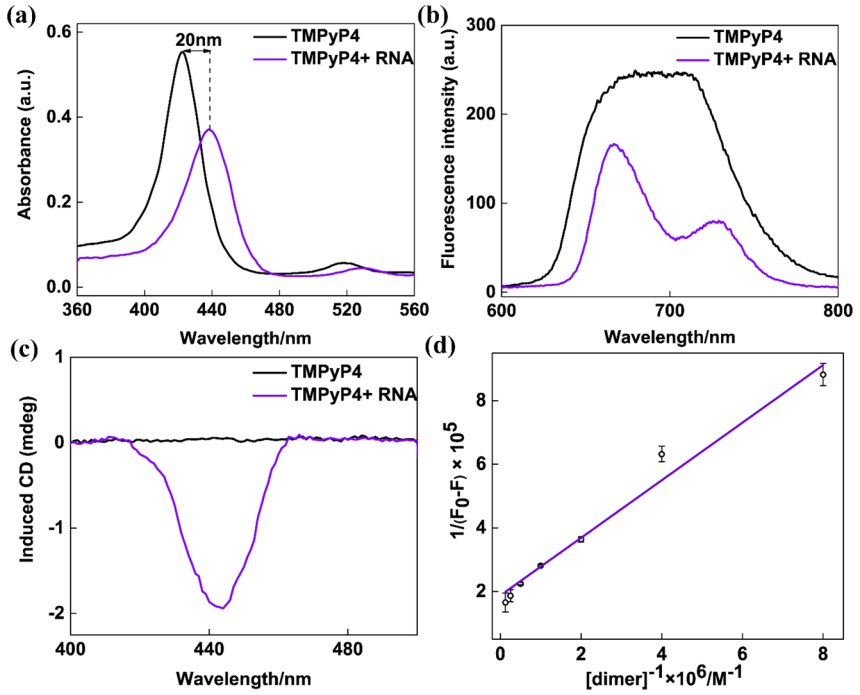

Figure 2. Steady-state (a) absorption spectra. (b) Fluorescence spectra of 2 μM TMPyP4 with/without 8 μM TERRA G-quadruplex dimer. (c) ICD spectra of 4 μM TMPyP4 and its complex with 16 μM TERRA G-quadruplex dimer. (d) Lineweaver−Burk curve for determining the binding constant via fluorescence titration method. The violet line represents the fitted data.

and fourth lanes corresponds to the 10-nt structure with the TERRA G-quadruplex dimer concentrations of 10 μM and 8 μM, respectively. The low concentration is the one used in the following experiments for binding with porphyrin, while the high concentration is the same as that used in previous experiments for verification of the current gel electrophoresis photograph method.[9,33] As expected, lanes 2 and 4 both migrate similarly to that of the 40-nt ssDNA marker, indicating the formation of the G-quadruplex dimer composed of four 10-nt r(GGGUUAGGGU) strands under the two concentrations. The CD results and gel electrophoresis analysis convincingly demonstrate that in our experimental conditions, the 10-nt r(GGGUUAGGGU) sequence exists in the unique form of a parallel-stranded G-quadruplex dimer. Additionally, gel electrophoresis analysis also shows that in the presence of TMPyP4, this TERRA G-quadruplex dimer (lanes 3 and 5) still stably exists. The addition of TMPyP4 does not lead to the collapse of the G-quadruplex dimer. After identification of the TERRA G-quadruplex dimer conformation, we performed the following experiments by multiple spectroscopic methods to examine the interaction between TMPyP4 and the TERRA G-quadruplex dimer. A large excess of RNA concentration relative to that of TMPyP4 (molar ratio of 4:1) was employed to ensure that all TMPyP4 molecules were bound to the TERRA G-quadruplex.

Multiple-Technique Spectroscopic Characterization of Binding Modes, Binding Stoichiometry, and Binding Constant. Figure 2a displays the steady-state UV−vis absorption spectra of TMPyP4 in the absence and presence of the TERRA G-quadruplex dimer. Free TMPyP4 displays a predominant absorption band at 421 nm. In the presence of the TERRA G-quadruplex dimer, TMPyP4 exhibits a redshift of 20 nm and hypochromicity degree of approximately 35% in the Soret band compared to the free TMPyP4. Generally speaking, for the interaction of TMPyP4 with DNA duplexes or DNA G-quadruplexes, the intercalation mode results in a large bathochromic shift (15 nm) and marked hypochromism

DOI: 10.1021/acs.jpclett.9b00637
J. Phys. Chem. Lett. 2019, 10, 2143−2150

(35%) in the porphyrin Soret band, whereas the external binding mode exhibits a smaller bathochromic shift (8 nm) and weaker hypochromism (10%).[34] In our case, given the large redshift (20 nm) and the pronounced hypochromicity (35%) of the Soret band, TMPyP4 should bind with the TERRA G-quadruplex dimer via the intercalation mode.

Figure 2b shows the fluorescence spectra of free TMPyP4 and its complex with the TERRA G-quadruplex dimer. As can be seen, free TMPyP4 presents a featureless broad emission spectrum from 630 to 780 nm. This is caused by the coupling of the first excited state S_1 with a nearby charge-transfer state (CT) from the porphyrin core to the pyridinium group. The coupling is favored in high-polarity solvents and can be facilitated by a high degree of rotational freedom of *N*-methylpyridinium and *N*-propylpyridinium groups. Upon binding with TERRA G-quadruplex dimer, this broad emission of TMPyP4 is split into two peaks of Q(0, 0) and Q(0, 1) bands with emission maxima at around 667 and 727 nm, and the ratio of intensity at 667 nm to that at 727 nm is also increased greatly. The splitting of the Q(0, 0) and Q(0, 1) bands indicates obviously the binding of porphyrins to TERRA G-quadruplex dimer within a low-polarity RNA microenvironment, and there is confinement of porphyrin rotations within the binding sites. These two effects brought by binding with RNA thus render the electronic S_1−CT mixing less effective, causing the splitting of Q(0, 0) and Q(0, 1) bands.[35]

Figure 2c shows the induced circular dichroism (ICD) spectra for TMPyP4 with TERRA G-quadruplex. Although many ligands are achiral and optically inactive, they can acquire ICD signals upon interaction with nucleic acids. The observation of an ICD signal for the absorption bands of the achiral ligand is indicative of an interaction of the ligand with nucleic acid. For the achiral porphyrin TMPyP4, its negative induced CD signal in the Soret band is characteristic of the intercalation mode, whereas its positive induced CD bands (or no signal at all) are usually indicators of external binding.[36] As shown in Figure 2c, TMPyP4 does not display a CD signal in the absence of the TERRA G-quadruplex dimer. Upon complexation with the TERRA G-quadruplex dimer, a negative CD band at 440 nm is observed, indicating the intercalation mode in agreement with the results of UV−vis absorption and fluorescence spectroscopy.

As indicated by the steady-state spectroscopic results above, the intercalation mode might be involved in the binding of TMPyP4 with the TERRA G-quadruplex dimer. In principle, TMPyP4 can intercalate into two adjacent G-tetrads within a G-quadruplex block or at the 5′-5′ stacking interface between two G-quadruplex blocks. Do these intercalation events occur simultaneously, or is one of intercalative sites preferred? Are there any other binding sites or modes in addition to intercalation? The steady-state spectroscopy results should reflect mainly the features of the dominant binding mode, while the features due to the minor mode might be buried and not discerned. To further differentiate the possible binding modes, we performed the following transient absorption spectroscopy experiments that utilize the triplet excited state of TMPyP4 as a sensitive reporter to monitor and distinguish the G-quadruplex−ligand interaction modes.[37] This triplet reporter method is based on the fact that the triplet lifetime of the ligand is highly sensitive to the bound microenvironment, which could screen the triplet state from being quenched by oxygen molecules in bulk solution.

Figure 3a plots transient UV−vis absorption spectra of free TMPyP4 and TMPyP4 bound with the TERRA G-quadruplex

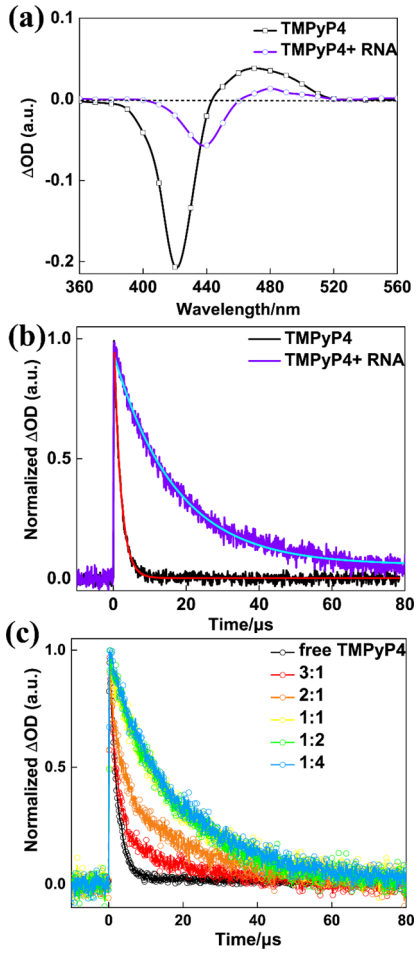

Figure 3. (a) Transient absorption spectra instantaneously (50 ns) after laser flash photolysis upon 355 nm excitation for free TMPyP4(2 μM) and its complex with 8 μM TERRA G-quadruplex dimer. (b) Normalized triplet decay signals of TMPyP4 (2 μM) in the absence (black) and presence (violet) of 8 μM TERRA G-quadruplex dimer. Fitted curves are shown by red and blue solid lines, respectively. (c) Normalized triplet decay signals for free TMPyP4 (black line) and [TMPyP4]/[quadruplex dimer] molar ratios (3:1, 2:1, 1:1, 1:2, and 1:4) are displayed with red, orange, yellow, green, and blue lines, respectively. All spectra and kinetics were recorded under aerobic conditions.

dimer. For free TMPyP4, transient absorptions owing to triplet excited-state formation (positive peak at 470 nm) and ground-state depletion (negative peak at 420 nm) were observed after laser flash photolysis upon 355 nm excitation. For TMPyP4 bound with TERRA G-quadruplex dimer, redshifts and hypochromicity can also be observed for both the ground-state depletion and triplet absorption bands in the transient absorption spectra. In this case, the triplet decay kinetics of free TMPyP4 and the TMPyP4/quadruplex dimer were monitored at 470 and 480 nm, respectively.

Figure 3b displays triplet decay curves for free TMPyP4 and its complex with TERRA G-quadruplex dimer. Triplet signals of free TMPyP4 follow a single-exponential decay with a lifetime of 1.8 ± 0.01 μs, which is in accordance with previous reports.[37] When binding with the TERRA G-quadruplex dimer, the triplet decay of TMPyP4 becomes remarkably

DOI: 10.1021/acs.jpclett.9b00637
J. Phys. Chem. Lett. 2019, 10, 2143−2150

slower but still follows a monoexponential law with a longer lifetime component of 18.8 ± 0.2 μs. The double-exponential function simply yielded poor fitting to the experimental data. The prolonged triplet decay lifetime indicates that TMPyP4 is bound within the RNA G-quadruplex microenvironment, which protects the triplet excited state from being quenched by oxygen molecules. Accordingly, the monoexponential decay observed in this work should be associated only with one type of bound microenvironment.[38] In other words, the interaction between TMPyP4 and the TERRA G-quadruplex dimer involves only a single binding mode.

Previous studies indicated that the triplet lifetime of TMPyP4 intercalated within duplex DNA was 27.8 μs for B-DNA and 28.6 μs for Z-DNA.[39] For TMPyP4 binding with DNA G-quadruplex, two triplet lifetime components of ∼28 and ∼3 μs were observed, corresponding to the population of intercalation between two neighboring G-tetrads and end-stacking on the terminal G-tetrad because the intercalation provided a well-protected microenvironment to prevent the O_2 quenching and the end-stacking had only a limited protection.[37] It is noticeable here that the triplet lifetime of 18.8 ± 0.2 μs for TMPyP4 binding with RNA G-quadruplex is shorter than the typical intercalative lifetime (∼28 μs), indicating that it should correspond to a binding site that can render a moderate degree of protection for TMPyP4. As shown in Scheme 2, the 5′-5′ stacking interface of two G-quadruplex blocks on each other at their 5′-ends is most likely to be such a binding site.[40] The 5′-5′ stacking interface between two blocks can allow TMPyP4 to be intercalated; however, it is expected to provide less confinement than the room between two adjacent G-tetrads of a G-quadruplex block. In a G-quadruplex block, two successive G-tetrads are linked by sugar−phosphates backbones through a phosphodiester bond. In contrast, in the stacking interface, each 5′-end belongs to its respective G-quadruplex block, so there are no chemical bonds formed between sugar−phosphate backbones of the two 5′-ends. Moreover, because of repulsion forces of the same negative charges, the sugar−phosphate backbones on the outside of two 5′-ends tend to be more separated from each other. Therefore, such conformations of sugar−phosphate backbones probably lead to more exposure of the 5′-5′ stacking interface to bulk solution, compared with two adjacent G-tetrads within a G-quadruplex block. When TMPyP4 intercalates into the 5′-5′ stacking interface, its triplet state will be subject to less protection, resulting in a moderate triplet lifetime.

Additionally, binding stoichiometry and binding constant are also important factors for understanding the interaction. To obtain the binding stoichiometry of the TMPyP4/quadruplex dimer, extensive triplet decay kinetics experiments were performed under a series of molar ratios of [TMPyP4]/[quadruplex dimer], as were those for the 1:4 ratio. The normalized triplet decay curves are shown in Figure 3c, and the fitted data are listed in Table 1.

When the [TMPyP4]/[quadruplex dimer] molar ratio varies from 1:2 to 1:1, both decay curves follow a monoexponential law and their lifetime components are18.4 ± 0.2 and 18.7 ± 0.1 μs, respectively, similar to the result of molar ratio 1:4. This indicates that all the porphyrin molecules are bound to TERRA G-quadruplex dimer even if the molar ratio increases to 1:1. However, at higher molar ratios of 2:1, two lifetime values (1.8 ± 0.01 and 20.1 ± 0.4 μs) were required to obtain a reasonable fitting of the triplet decay signal, strongly implying

Table 1. Triplet Decay Lifetimes of TMPyP4 in Air-Saturated Buffer Solution of TMPyP4/Quadruplex Dimer[a]

[TMPyP4]/[qudruplex dimer]	triplet lifetimes of TMPyP4 (μs)
1:2	18.4 ± 0.2
1:1	18.7 ± 0.1
2:1	1.8 ± 0.01 (60%)
	20.1 ± 0.4 (40%)
3:1	1.8 ± 0.01 (84%)
	20.0 ± 0.6 (16%)

[a]The dimer concentrations were 4 μM, 2 μM, 1 μM and 0.67 μM. The triplet lifetimes were obtained from mono-exponential ($I = I_0 + A_1e^{-t/\tau_1}$) or biexponential fitting ($I = I_0 + A_1e^{-t/\tau_1} + A_2e^{-t/\tau_2}$). Pre-exponential factors for the two lifetime components yield the respective percentages of free TMPyP4 and TMPyP4 bound to quadruplex dimer (values shown in parentheses) for molar ratios of 3:1 and 2:1.

the existence of free TMPyP4 in solution, in addition to the TMPyP4 bound to G-quadruplex. The presence of free TMPyP4 means the number of TMPyP4 molecules that are bound to G-quadruplexes is already saturated at molar ratios of 2:1 and 3:1, and hence, the molar ratio of 1:1 is supposed to be the binding stoichiometry. To further verify the binding stoichiometry, we also performed the continuous variation analysis (Job plots).[33] As shown in Figure S1, the intersection points of two fitted lines for TMPyP4 in complex with TERRA G-quadruplex dimer is 0.5, corresponding to the stoichiometry of 1:1. The result is well consistent with the value obtained by triplet decays, confirming the binding stoichiometry of 1:1.

Based on the 1:1 binding stoichiometry model, fluorescence titrations were conducted to obtain the binding constant (shown in Figure S2).[41] The fluorescence quenching was initiated by [TMPyP4/quadruplex dimer] complex formation, which can be evaluated by eq 1:

$$(F_0 - F)^{-1} = F_0^{-1} + K^{-1}F_0^{-1}[Q]^{-1} \quad (1)$$

where [Q] indicates the concentration of TERRA G-quadruplex dimer; F_0 and F are the fluorescence intensities obtained from peak areas without and with quencher, respectively; K denotes the binding constant of TMPyP4 to TERRA G-quadruplex dimer, which can be calculated from the slope and intercept of the Lineweaver−Burk curve as shown in Figure 2d (K = intercept/slope). The analysis of the Lineweaver−Burk curve provides the binding constant for TMPyP4 with TERRA G-quadruplex dimer being (1.92 ± 0.03) × 10^6 M^{-1}, indicating a quite strong binding affinity.[42]

Unambiguous Identification of the Binding Site by NMR Spectroscopy. According to the single-exponential triplet decay kinetics and the moderately lengthened triplet lifetime, only one binding site exists and 5′-5 stacking interface between two G-quadruplex blocks could be the most likely binding site. To ascertain unambiguously the binding site, we performed NMR experiments taking advantage of its potent structural characterization ability. Figure 4a shows the NMR spectrum for the TERRA G-quadruplex dimer alone. The characteristic guanine imino proton peaks at 11.3 ppm G2 and 11.2 ppm G8 for the middle G-tetrad, and 11.2 ppm G3 and G9 for the 3′-end G-tetrad, agree with the features for G-quadruplex formation.[9] Because of the G-quadruplex dimer formation, the imino proton peaks of the 5′-end G-tetrad are distinguishable from those of the 3′-end G-tetrad, displaying peaks at 10.6 ppm for G7 and 10.5 ppm for G1, which is characteristic for the

DOI: 10.1021/acs.jpclett.9b00637
J. Phys. Chem. Lett. 2019, 10, 2143−2150

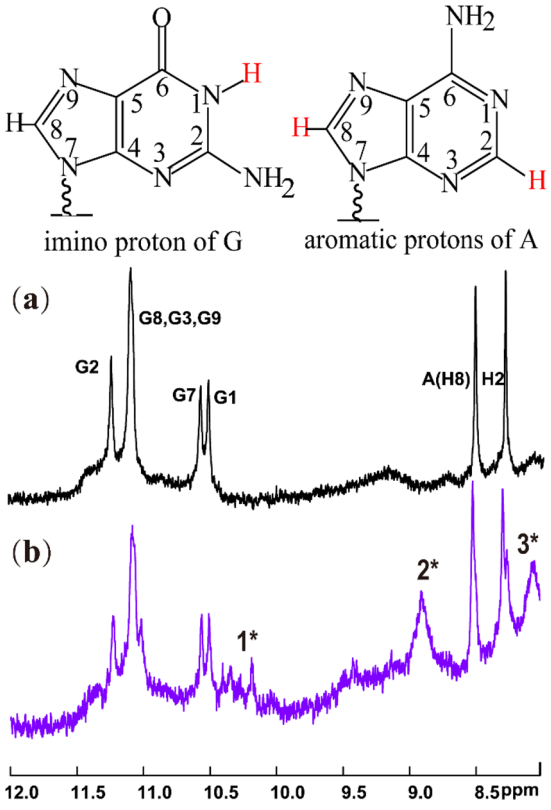

Figure 4. NMR spectra for 10-nt human telomeric RNA sequence r(GGGUUAGGGU) in K^+ buffer solution containing 90% H_2O and 10% D_2O: (a) TERRA G-quadruplex dimer; (b) TMPyP4/quadruplex dimer. G-quadruplex dimer concentration: 200 μM; TMPyP4 concentration: 50 μM.

TERRA G-quadruplex dimer. Furthermore, the adenine A aromatic protons' peaks at 8.5 ppm (H8) and 8.3 ppm (H2) are observed, which is consistent with the formation of A·(G·G·G·G)·A hexad of the 5′-5′ stacking interface between two G-quadruplex blocks and in accordance with previous assignments.[28] In principle, if the binding of ligands to G-quadruplexes could cause broadening and/or shift of the proton peaks neighboring to the binding site, the ligand binding site can be identified by well-resolved protons of the G-quadruplex.[43] As shown in Figure 4b, upon addition of TMPyP4 to TERRA G-quadruplex dimer solution, imino proton peaks of the 3′-end G-tetrad residues (G3 and G9) and the middle G-tetrad residues (G2 and G8) are unaffected in general. In contrast, the peaks of imino protons of the 5′-end A·(G·G·G·G)·A hexad's residues (G1 and G7) and aromatic protons of A(H8/H2) are most perturbed, broadened, and shifted upfield by ∼0.2 ppm, with emergence of 1* peaks for the imino protons of G1/G7 and 3* peaks for the aromatic protons of A(H8/H2). These observations demonstrate clearly that the ligand TMPyP4 binds between the 5′-5′ stacking interface of two G-quadruplex blocks, whereas the possibility of end-stacking on the 3′-end G-tetrad or intercalation between middle G-tetrad of a G-quadruplex block can be ruled out. Additionally, the 2* peak for porphyrin protons upon binding with G-quadruplex is also broadened and upfield shifted in comparison to the free porphyrin (see Figure S3c).[44]

Such a neat binding mode can be rationalized by previous knowledge of the structure of this TERRA G-quadruplex dimer.[28] On one hand, each G-quadruplex block adopts a parallel-stranded propeller-type fold with four medium-sized grooves, two of which are occupied by a UUA double-chain reversal loop. The adenines in the UUA loops are facing toward the G-tetrad core, and the U4 uracils are also facing toward the core, while the U5 uracils are pointing outside (Scheme 1a). This arrangement results in a very compact and rigid structure, which cannot offer sufficient room to accommodate porphyrin and thus is unfavorable for the intercalation mode between two G-tetrads of a single G-quadruplex block. On the other hand, there is decreased steric hindrance of sugar−phosphate backbones at the dimeric 5′-5′ stacking interface of two G-quadruplex blocks. Furthermore, the adenines in the UUA linkers are nearly coplanar with the 5′-end G-tetrad, forming an A·(G·G·G·G)·A hexad, which can enlarge the $\pi-\pi$ stacking plane and provide an attractive binding site for the π-ligand porphyrin. Hence, TMPyP4 prefers intercalating into the 5′-5′ stacking interface of two G-quadruplex blocks. Meanwhile, according to the TERRA G-quadruplex dimer structure, there are two uracil residues in each G-quadruplex block stacked on the 3′-end G-tetrad core. The uracil overhang at the 3′-end should hinder the $\pi-\pi$ stacking between TMPyP4 and the 3′-end G-tetrad, and thus the absence of end-stacking mode can be understood.

In summary, by the coupling of multiple steady-state and time-resolved spectroscopy analyses with NMR methods, the binding interaction of TMPyP4 with the native TERRA G-quadruplex dimer is thoroughly investigated. The large redshift and hypochromicity of the Soret absorption band, splitting of fluorescence band, and negative ICD band suggest the existence of the intercalation mode. The transient absorption spectroscopy results further ascertain the existence of one binding site and determine the binding stoichiometry to be 1:1, showing a single-exponential triplet decay lifetime of 18.8 ± 0.2 μs for the TMPyP4 bound with the TERRA G-quadruplex dimer. Intriguingly, the NMR spectra reveal the pronounced upfield shifts of proton peaks for the 5′-end A·(G·G·G·G)·A hexad's G residues and A residues, but not for the middle G-tetrad or 3′-end G-tetrad, thus unambiguously identify the 5′-5′ stacking interface of the TERRA G-quadruplex dimer to be the only binding site. The preferential binding of π-ligand porphyrin onto this 5′-5′ stacking dimeric interface is consistent with the structural feature of the enlarged $\pi-\pi$ stacking plane of the A·(G·G·G·G)·A hexad. Given the fact that it is common for RNA G-quadruplex to adopt higher-order structures through 5′-5′stacking interface, the ligand intercalation into the dimeric 5′-5′ stacking interface could be ubiquitous. These findings provide mechanistic insights for screening optimal RNA G-quadruplex binders and development of anticancer drugs or probes targeting higher-order arrangements of G-quadruplexes in long TERRA sequences.

■ ASSOCIATED CONTENT

Supporting Information

The Supporting Information is available free of charge on the ACS Publications website at DOI: 10.1021/acs.jpclett.9b00637.

Experimental materials and methods, Job plot, fluorescence titration data, and NMR data of free porphyrin (PDF)

DOI: 10.1021/acs.jpclett.9b00637
J. Phys. Chem. Lett. 2019, 10, 2143−2150

AUTHOR INFORMATION

Corresponding Authors

*E-mail: hongmei@bnu.edu.cn (H.S.).
*E-mail: songdi@iccas.ac.cn (D.S.).
*E-mail: yangchunfan@bnu.edu.cn (C.Y.).

ORCID

Hongmei Su: 0000-0001-7384-6523

Notes

The authors declare no competing financial interest.

ACKNOWLEDGMENTS

This work was financially supported by the National Natural Science Foundation of China (Grant Nos. 21425313, 21727803, 21703011, and 21773257).

REFERENCES

(1) Burge, S.; Parkinson, G. N.; Hazel, P.; Todd, A. K.; Neidle, S. Quadruplex DNA: Sequence, Topology and Structure. *Nucleic Acids Res.* **2006**, *34*, 5402−5415.

(2) Sacca, B.; Lacroix, L.; Mergny, J. L. The Effect of Chemical Modifications on the Thermal Stability of Different G-Quadruplex-Forming Oligonucleotides. *Nucleic Acids Res.* **2005**, *33*, 1182−1192.

(3) Azzalin, C. M.; Reichenbach, P.; Khoriauli, L.; Giulotto, E.; Lingner, J. Telomeric Repeat Containing Rna and Rna Surveillance Factors at Mammalian Chromosome Ends. *Science* **2007**, *318*, 798−801.

(4) Kumari, S.; Bugaut, A.; Huppert, J. L.; Balasubramanian, S. An Rna G-Quadruplex in the 5′ Utr of the Nras Proto-Oncogene Modulates Translation. *Nat. Chem. Biol.* **2007**, *3*, 218−221.

(5) Arora, A.; Maiti, S. Differential Biophysical Behavior of Human Telomeric Rna and DNA Quadruplex. *J. Phys. Chem. B* **2009**, *113*, 10515−10520.

(6) Collie, G. W.; Haider, S. M.; Neidle, S.; Parkinson, G. N. A Crystallographic and Modelling Study of a Human Telomeric Rna (Terra) Quadruplex. *Nucleic Acids Res.* **2010**, *38*, 5569−5580.

(7) Rouleau, S.; Jodoin, R.; Garant, J. M.; Perreault, J. P. Rna G-Quadruplexes as Key Motifs of the Transcriptome. *Adv. Biochem. Eng./Biotechnol.* **2017**, 1−20, DOI: 10.1007/10_2017_8.

(8) Garbett, N. C.; Ragazzon, P. A.; Chaires, J. B. Circular Dichroism to Determine Binding Mode and Affinity of Ligand-DNA Interactions. *Nat. Protoc.* **2007**, *2*, 3166−3172.

(9) Martadinata, H.; Phan, A. T. Structure of Propeller-Type Parallel-Stranded Rna G-Quadruplexes, Formed by Human Telomeric Rna Sequences in K^+ Solution. *J. Am. Chem. Soc.* **2009**, *131*, 2570−2578.

(10) Bugaut, A.; Rodriguez, R.; Kumari, S.; Hsu, S. T.; Balasubramanian, S. Small Molecule-Mediated Inhibition of Translation by Targeting a Native Rna G-Quadruplex. *Org. Biomol. Chem.* **2010**, *8*, 2771−2776.

(11) Patel, D. J.; Phan, A. T.; Kuryavyi, V. Human Telomere, Oncogenic Promoter and 5′-Utr G-Quadruplexes: Diverse Higher Order DNA and Rna Targets for Cancer Therapeutics. *Nucleic Acids Res.* **2007**, *35*, 7429−7455.

(12) Cammas, A.; Millevoi, S. Rna G-Quadruplexes: Emerging Mechanisms in Disease. *Nucleic Acids Res.* **2016**, *45*, 1584−1595.

(13) Ji, X.; Sun, H.; Zhou, H.; Xiang, J.; Tang, Y.; Zhao, C. Research Progress of Rna Quadruplex. *Nucleic Acid Ther.* **2011**, *21*, 185−200.

(14) Pandey, S.; Agarwala, P.; Maiti, S. Targeting RNA G-Quadruplexes for Potential Therapeutic Applications. *Top. Med. Chem.* **2017**, *27*, 177−206.

(15) Millevoi, S.; Moine, H.; Vagner, S. G-Quadruplexes in Rna Biology. *Wiley Interdiscip Rev. RNA* **2012**, *3*, 495−507.

(16) Dai, J.; Carver, M.; Hurley, L. H.; Yang, D. Solution Structure of a 2:1 Quindoline-C-Myc G-Quadruplex: Insights into G-Quadruplex-Interactive Small Molecule Drug Design. *J. Am. Chem. Soc.* **2011**, *133*, 17673−17680.

(17) Collie, G. W.; Promontorio, R.; Hampel, S. M.; Micco, M.; Neidle, S.; Parkinson, G. N. Structural Basis for Telomeric G-Quadruplex Targeting by Naphthalene Diimide Ligands. *J. Am. Chem. Soc.* **2012**, *134*, 2723−2731.

(18) Joachimi, A.; Benz, A.; Hartig, J. S. A Comparison of DNA and Rna Quadruplex Structures and Stabilities. *Bioorg. Med. Chem.* **2009**, *17*, 6811−6815.

(19) Pérez-Arnaiz, C.; Busto, N.; Santolaya, J.; Leal, J. M.; Barone, G.; García, B. Kinetic Evidence for Interaction of Tmpyp4 with Two Different G-Quadruplex Conformations of Human Telomeric DNA. *Biochim. Biophys. Acta, Gen. Subj.* **2018**, *1862*, 522−531.

(20) Ali, A.; Bansal, M.; Bhattacharya, S. Ligand 5,10,15,20-Tetra(N-Methyl-4-Pyridyl)Porphine (Tmpyp4) Prefers the Parallel Propeller-Type Human Telomeric G-Quadruplex DNA over Its Other Polymorphs. *J. Phys. Chem. B* **2015**, *119*, 5−14.

(21) Chen, M.; Song, G.; Wang, C.; Hu, D.; Ren, J.; Qu, X. Small-Molecule Selectively Recognizes Human Telomeric G-Quadruplex DNA and Regulates Its Conformational Switch. *Biophys. J.* **2009**, *97*, 2014−2023.

(22) Wang, J.; Chen, Y.; Ren, J.; Zhao, C.; Qu, X. G-Quadruplex Binding Enantiomers Show Chiral Selective Interactions with Human Telomere. *Nucleic Acids Res.* **2014**, *42*, 3792−3802.

(23) Zhang, D. H.; Fujimoto, T.; Saxena, S.; Yu, H. Q.; Miyoshi, D.; Sugimoto, N. Monomorphic Rna G-Quadruplex and Polymorphic DNA G-Quadruplex Structures Responding to Cellular Environmental Factors. *Biochemistry* **2010**, *49*, 4554−4563.

(24) Xu, Y.; Kaminaga, K.; Komiyama, M. G-Quadruplex Formation by Human Telomeric Repeats-Containing Rna in Na^+ Solution. *J. Am. Chem. Soc.* **2008**, *130*, 11179.

(25) Malgowska, M.; Czajczynska, K.; Gudanis, D.; Tworak, A.; Gdaniec, Z. Overview of the Rna G-Quadruplex Structures. *Acta Biochim Pol* **2017**, *63*, 609−621.

(26) Collie, G. W.; Parkinson, G. N.; Neidle, S.; Rosu, F.; De Pauw, E.; Gabelica, V. Electrospray Mass Spectrometry of Telomeric Rna (Terra) Reveals the Formation of Stable Multimeric G-Quadruplex Structures. *J. Am. Chem. Soc.* **2010**, *132*, 9328−9334.

(27) Collie, G. W.; Sparapani, S.; Parkinson, G. N.; Neidle, S. Structural Basis of Telomeric Rna Quadruplex–Acridine Ligand Recognition. *J. Am. Chem. Soc.* **2011**, *133*, 2721−2728.

(28) Martadinata, H.; Phan, A. T. Structure of Human Telomeric Rna (Terra): Stacking of Two G-Quadruplex Blocks in K(+) Solution. *Biochemistry* **2013**, *52*, 2176−2183.

(29) Han, H.; Langley, D. R.; Rangan, A.; Hurley, L. H. Selective Interactions of Cationic Porphyrins with G-Quadruplex Structures. *J. Am. Chem. Soc.* **2001**, *123*, 8902−8913.

(30) Qin, Y.; Rezler, E. M.; Gokhale, V.; Sun, D.; Hurley, L. H. Characterization of the G-Quadruplexes in the Duplex Nuclease Hypersensitive Element of the Pdgf-a Promoter and Modulation of Pdgf-a Promoter Activity by Tmpyp4. *Nucleic Acids Res.* **2007**, *35*, 7698−7713.

(31) Freyer, M. W.; Buscaglia, R.; Kaplan, K.; Cashman, D.; Hurley, L. H.; Lewis, E. A. Biophysical Studies of the C-Myc Nhe Iii1 Promoter: Model Quadruplex Interactions with a Cationic Porphyrin. *Biophys. J.* **2007**, *92*, 2007−2015.

(32) Mikami-Terao, Y.; Akiyama, M.; Yuza, Y.; Yanagisawa, T.; Yamada, O.; Yamada, H. Antitumor Activity of G-Quadruplex-Interactive Agent Tmpyp4 in K562 Leukemic Cells. *Cancer Lett.* **2008**, *261*, 226−234.

(33) Yao, X.; Song, D.; Qin, T.; Yang, C.; Yu, Z.; Li, X.; Liu, K.; Su, H. Interaction between G-Quadruplex and Zinc Cationic Porphyrin: The Role of the Axial Water. *Sci. Rep.* **2017**, *7*, 10951.

(34) Qin, T.; Liu, K.; Song, D.; Yang, C.; Su, H. Porphyrin Bound to I-Motifs: Intercalation Versus External Groove Binding. *Chem. - Asian J.* **2017**, *12*, 1578−1586.

(35) Wei, C.; Jia, G.; Zhou, J.; Han, G.; Li, C. Evidence for the Binding Mode of Porphyrins to G-Quadruplex DNA. *Phys. Chem. Chem. Phys.* **2009**, *11*, 4025−4032.

(36) D'Urso, A.; Nardis, S.; Pomarico, G.; Fragalà, M. E.; Paolesse, R.; Purrello, R. Interaction of Tricationic Corroles with Single/

DOI: 10.1021/acs.jpclett.9b00637
J. Phys. Chem. Lett. 2019, 10, 2143−2150

Double Helix of Homopolymeric Nucleic Acids and DNA. *J. Am. Chem. Soc.* **2013**, *135*, 8632−8638.
(37) Song, D.; Yang, W.; Qin, T.; Wu, L.; Liu, K.; Su, H. Explicit Differentiation of G-Quadruplex/Ligand Interactions: Triplet Excited States as Sensitive Reporters. *J. Phys. Chem. Lett.* **2014**, *5*, 2259−2266.
(38) Keane, P. M.; Kelly, J. M. Transient Absorption and Time-Resolved Vibrational Studies of Photophysical and Photochemical Processes in DNA-Intercalating Polypyridyl Metal Complexes or Cationic Porphyrins. *Coord. Chem. Rev.* **2018**, *364*, 137−154.
(39) Qin, T. X.; Liu, K. H.; Song, D.; Yang, C. F.; Zhao, H. M.; Su, H. M. Binding Interactions of Zinc Cationic Porphyrin with Duplex DNA: From B-DNA to Z-DNA. *Int. J. Mol. Sci.* **2018**, *19*, 1071.
(40) Kettani, A.; Gorin, A.; Majumdar, A.; Hermann, T.; Skripkin, E.; Zhao, H.; Jones, R.; Patel, D. J. A Dimeric DNA Interface Stabilized by Stacked A.(G.G.G.G).A Hexads and Coordinated Monovalent Cations. *J. Mol. Biol.* **2000**, *297*, 627−644.
(41) Cui, F. L.; Wang, J. L.; Cui, Y. R.; Li, J. P. Fluorescent Investigation of the Interactions between N-(P-Chlorophenyl)-N'-(1-Naphthyl) Thiourea and Serum Albumin: Synchronous Fluorescence Determination of Serum Albumin. *Anal. Chim. Acta* **2006**, *571*, 175−183.
(42) Bai, L.-P.; Liu, J.; Han, L.; Ho, H.-M.; Wang, R.; Jiang, Z.-H. Mass Spectrometric Studies on Effects of Counter Ions of Tmpyp4 on Binding to Human Telomeric DNA and Rna G-Quadruplexes. *Anal. Bioanal. Chem.* **2014**, *406*, 5455−5463.
(43) Phan, A. T.; Kuryavyi, V.; Gaw, H. Y.; Patel, D. J. Small-Molecule Interaction with a Five-Guanine-Tract G-Quadruplex Structure from the Human Myc Promoter. *Nat. Chem. Biol.* **2005**, *1*, 167−173.
(44) Morris, M. J.; Wingate, K. L.; Silwal, J.; Leeper, T. C.; Basu, S. The Porphyrin Tmpyp4 Unfolds the Extremely Stable G-Quadruplex in Mt3-Mmp Mrna and Alleviates Its Repressive Effect to Enhance Translation in Eukaryotic Cells. *Nucleic Acids Res.* **2012**, *40*, 4137−4145.

DOI: 10.1021/acs.jpclett.9b00637
J. Phys. Chem. Lett. 2019, 10, 2143−2150